Bioorganic & Medicinal Chemistry Letters 23 (2013) 188–193

Contents lists available at SciVerse ScienceDirect

Bioorganic & Medicinal Chemistry Letters

journal homepage: www.elsevier.com/locate/bmcl

Triazoyl–phenyl linker system enhancing the aqueous solubility of a molecular probe and its efficiency in affinity labeling of a target protein for jasmonate glucoside

Satoru Tamura [a], Sho Inomata [a], Makoto Ebine [a], Takahisa Genji [a], Izumi Iwakura [b], Makoto Mukai [a], Mitsuru Shoji [c], Takeshi Sugai [c], Minoru Ueda [a,*]

[a] Department of Chemistry, Tohoku University, 6-3 Aramaki-aza Aoba, Aoba-ku, Sendai 980-8578, Japan
[b] Faculty of Engineering, Kanagawa University, 3-27-1 Rokkakubashi, Kanagawa-ku, Yokohama 221-8686, Japan
[c] Faculty of Pharmacy Keio University, 1-5-30 Shibakoen, Minato-ku, Tokyo 105-8512, Japan

ARTICLE INFO

Article history:
Received 4 September 2012
Revised 4 October 2012
Accepted 29 October 2012
Available online 6 November 2012

Keywords:
Molecular probe
Linker
CuAAC
TAzP
Target protein

ABSTRACT

In methods employing molecular probes to explore the targets of bioactive small molecules, long or rigid linker moieties are thought to be critical factors for efficient tagging of target protein. We previously reported the synthesis of a jasmonate glucoside probe with a highly rigid linker consisting of a triazoyl–phenyl (TAzP) moiety, and this probe demonstrated effective target tagging. Here we compare the TAzP probe with other rigid or flexible probes with respect to target tagging efficiency, hydrophobic parameters, aqueous solubility, and dihedral angles around the biaryl linkage by a combination of empirical and calculation methods. The rigid biaryl linkage of the TAzP probe has a skewed conformation that influences its aqueous solubility. Such features that include rigidness and good aqueous solubility resulted in highly efficient target tagging. These findings provide a promising guideline toward designing of better linkers for improving molecular probe performance.

Molecular probes are recognized as powerful tools for exploring the targets of bioactive small molecules.[1–3] An appropriately designed molecular probe affords highly efficient chemical tagging of target proteins. A molecular probe consists of four essential components: a pharmacophore, reactive functionality, a molecular tag, and a linker moiety (Fig. 1). Among these, the selection of a linker of the appropriate length and structure strongly affects the efficiency of target tagging (Fig. 1).[4–7] In general, it is considered that the role of the linker is to cast the molecular tag away from pharmacophore, which is an essential unit for binding with a specific target.[8] It is generally accepted that the longer or more rigid the linker is, the more effective the casting process.[9] To date, substantial attention has been paid to the design of the linker. Polymethylene,[9] oligopeptides, including polyglycine[10] or polyproline-rod,[5] and polyethyleneglycol (PEG)[11,12] are widely used as standard linkers (Fig. 1). However, a long linker causes serious issues associated with its hydrophobic nature. An increase in hydrophobicity is accompanied by a decrease in aqueous solubility as well as an increase in nonspecific binding.[6,13] Thus, a linker that combines rigidness for effective casting of the molecular tag with high aqueous solubility is strongly desired.

Recently, we reported the potency of a molecular probe (**1**) having a highly rigid triazoyl–phenyl (TAzP)[14] linker designed for efficient affinity tagging of the membrane target of jasmonate glucoside (**2**[16] in Fig. 2) (MTJG).[10,15] Surprisingly, even a short TAzP linker functioned well and provided useful target tagging. The TAzP probe can be easily constructed by copper-catalyzed azide alkyne cycloaddition (CuAAC)[17–19] between an alkyl azide and aryl acetylene, and it provided better results for tagging the corresponding target protein than the conventional molecular probe. In this study, we will discuss the chemical basis for the high efficiency of the TAzP linker and report our findings that the TAzP linker confers rigidness as well as good aqueous solubility to a molecular probe because of its skewed conformation around the biaryl linkage.

TAzP molecular probe **1** possesses a biaryl structure substituted by a pharmacophore and a large tag at each end of the unit (Fig. 2). In a previous study, we hypothesized that the reason for the favorable performance of the TAzP probe might be attributed to the rigidness of the biaryl structure, which functions to cast the tag away from the pharmacophore. Novel insight regarding the proficiency of the TAzP linker can contribute to the development of other high-performance linkers. However, our hypothesis has remained unproven because of a lack of appropriate control experiments. To resolve this deficiency, we designed and synthesized alkyne units **9**–**12** (Schemes S1–S4, Supplementary data), which provide 'CuAAC'-prepared probes **3**, **4**, **6**, and **7** (Figs. 2 and 3). Each alkyne unit (**9**–**12**)

* Corresponding author.
E-mail address: ueda@m.tohoku.ac.jp (M. Ueda).

0960-894X/$ - see front matter © 2012 Elsevier Ltd. All rights reserved.
http://dx.doi.org/10.1016/j.bmcl.2012.10.124

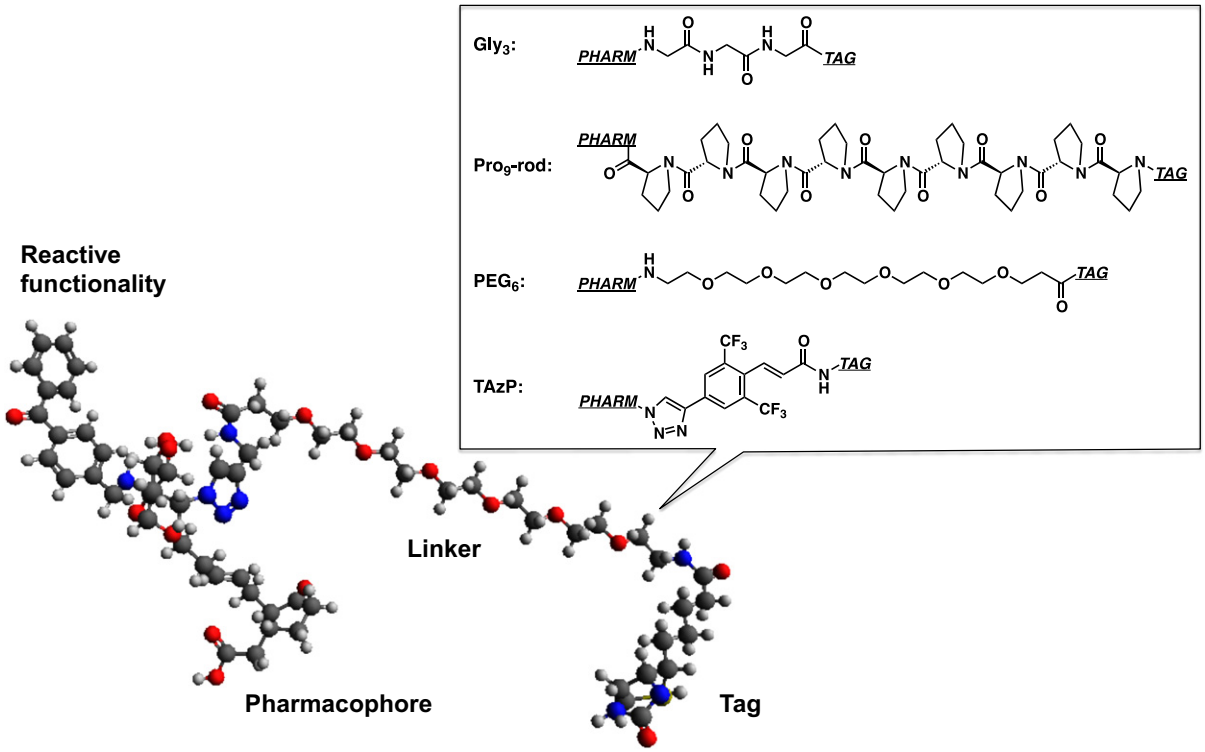

Figure 1. A ball-and-stick model of **5** consisting of four essential components: a pharmacophore, reactive functionality, a molecular tag, and a linker moiety. Structures of conventional linkers are also shown (framed rectangle).

was coupled with azide-JAG (**13**)[14,20] under CuAAC conditions using tris(3-hydroxypropyltriazolylmethyl)amine (THPTA)[21,22] as a catalyst. The resulting probes were used as appropriate controls for TAzP probe **1** in the following experiments.

According to our hypothesis,[14] the advantage of the TAzP linker is lost when its planarity is disrupted by the introduction of methylene units between the triazole and aryl rings (Fig. 2). Thus, we designed ethyl-tethered probe **3**, in which the C2-unit in **1**, encompassing the α,β-positions of the carbonyl group, was shifted to the position between the triazole and aryl groups. Probe **3** has the same linker length (14 atoms) as **1** (Fig. 2) and is a useful control for comparison with **1**. We also synthesized alkyne units **11** and **12**, which provided the triazoylquinolyl (TAzQ) probes **6** and **7**, respectively. Higher planarity can be anticipated for the biaryl group of **6** and **7** than for the corresponding moiety of **1**. The nitrogen atom in the quinoline ring in **6** and **7** serves to lower the hydrophobicity of the corresponding probe despite the large size of this aromatic ring.[23] In addition, alkyne unit **10** with a hexa-PEG linker provided probe **4** by possessing the long PEG fragment, which added flexibility as compared to the rigid TAzP probe (Fig. 2).

First, we compared the efficiencies in target tagging among ethyl-tethered probe **3**, TAzQ probes (**6** and **7**), PEG-substituted probe **4**, conventional triglycyl probe **5**[10], and TAzP probe **1**. The efficiency of each probe was assessed by the photoaffinity-based target tagging experiment with MTJG.[15] MTJG has been identified as a target protein for the leaf-closing factor of *Samanea saman* (**2**).[16,24,25] Photoaffinity labeling by each probe was performed using the motor cell of *S. saman*,[10,14] and the prepared membrane fractions were subjected to SDS–PAGE analysis with labeled MTJG. The preparation and subsequent utilization of *Samanea* protoplasts in photoaffinity labeling experiments were performed according to the procedures described in our previous study.[14] Unexpectedly, TAzP probe **1** provided the highest tagging efficiency among all the probes (**1** and **3**–**7**) followed by triglycyl-linked probe **5** (Fig. 4). Conversely, all of the remaining probes, including TAzQ, did not provide any band corresponding to biotinylated MTJG (Fig. 4).

Because ethyl-tethered probe **3** with the same linker length (14 atoms) as **1** does not show a band for tagged MTJG, it can be concluded that the efficient photoaffinity tagging by **1** is not related to the length of the linker but depends on the chemical nature of the biaryl structure in the TAzP linker. This result suggests that the advantage of the rigid TAzP linker might lie in its ability to effectively cast the large tag away from the pharmacophore.

This advantage of the rigid TAzP linker was also supported by the fact that hexa-PEG probe **4** equipped with a linker extending 27 atoms in length does not show a band for tagged MTJG. Hydrophilic and flexible PEG linkers are expected to adopt an extended conformation, in which the tag is effectively cast away from the pharmacophore, whereas experimental and theoretical studies suggest that low molecular weight PEG oligomers/polymers predominantly adopt a helical conformation in an aqueous environment.[26–28] A helical conformation of the PEG linker would confine the large tag close to the pharmacophore and sometimes cause aggregation with the attached pharmacophore.[27] Thus, this drawback of the PEG linker could be responsible for the disappointing results for hexa-PEG probe **4**. It is also important to determine whether nonspecific binding to proteins other than MTJG occurred using PEG-linked **4** (data not shown). It is reported that the use of a long PEG linker in affinity-based protein purification cannot suppress the incorporation of nonspecific proteins.[6,13] These results suggest that increasing the length of the linker would not be an effective strategy.

Interestingly, no biotinylated MTJG was found in photoaffinity labeling experiments using TAzQ probe **6** or **7**. As it is expected that the TAzQ linker affords planarity and rigidness equal to or greater than the TAzP linker, we suspected that an unknown chemical property of TAzP might be responsible for its notable target affinity.

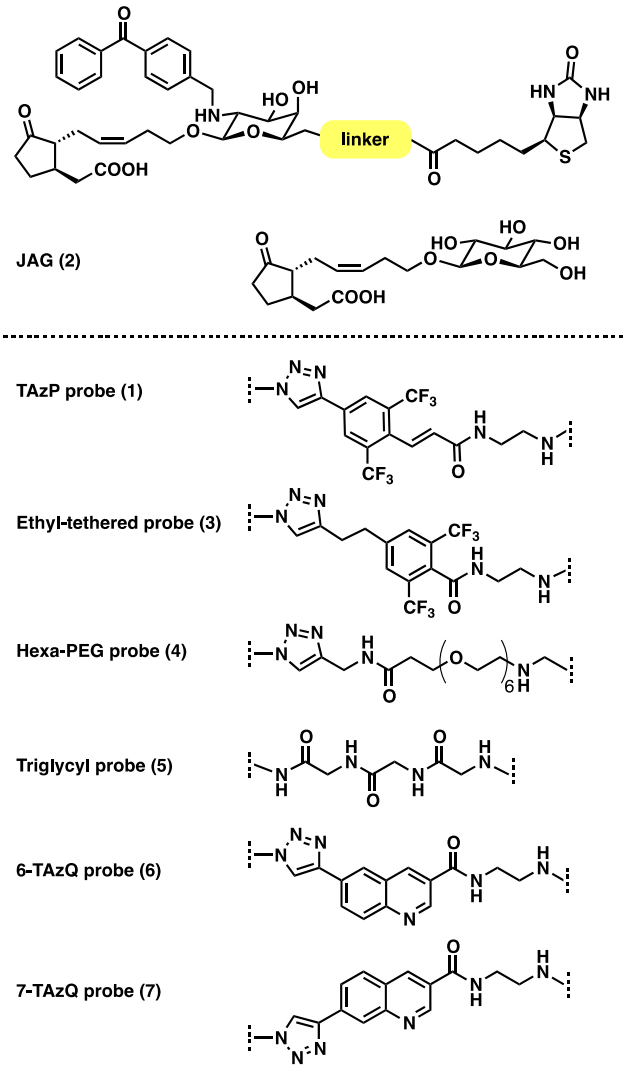

Figure 2. Structures of synthetic probes (**1** and **3**–**7**) and parent ligand JAG (**2**).

The structural modifications to parent ligand **2** required for its conversion into various synthetic probes afford dramatic changes in the physicochemical properties of **2** and cause a decrease in its target affinity. As parent ligand **2** is highly soluble in aqueous media, it is expected that the poor aqueous solubility of a 'CuAAC'-prepared probe might decrease its availability for formation of an adduct in photoaffinity tagging using living cells. Therefore, the reason for the differences in target affinity among **1** and **3**–**7** might be identified by an assessment of aqueous solubility.

In general, the aqueous solubility of a small molecule depends on its hydrophobicity. Thus, we examined the hydrophobicity parameters (calculated log *P* and retention time on reversed phase (RP)-HPLC) and aqueous solubility of probes (**1** and **3**–**7**). Both calculated log *P* (*C*Log P)[29–31] and retention time in reversed phase RP-HPLC are widely used to assess the hydrophobicity of small molecules. All the *C*Log *P* values for probes **1** and **3**–**7** were much higher than that of parent ligand **2** (*C*Log *P* = −0.39) (Table 1). Among them, the *C*Log *P* value of TAzP probe **1** was the highest and was equivalent to that of **3**. TAzQ probes **6** and **7** have medium values, and the values for **4** and **5** are the lowest. The rank order of the *C*Log *P* values (**3** ≃ **1** > **6** = **7** > **4** > **5**) strongly correlated with that of the retention times in RP-HPLC (**1** > **3** > **7** > **6** > **4** > **5**) (Table 1). These data suggest the following rankorder of hydrophobicity (**3** ≃ **1** > **6** ≃ **7** > **4** > **5**). Interestingly, no clear relationship was found between aqueous solubility and hydrophobicity (Table 1). The rank order of aqueous solubility (**5** ≫ **4** > **3** ≃ **1** > **7** ≃ **6**) suggested that the most hydrophobic pair (**1** and **3**) have greater aqueous solubility than that indicated from the hydrophobicity.

The successful tagging of the target by **5** is highly correlated with its exceptional aqueous solubility as well as its low hydrophobicity, which is similar to that of parent compound **2**. The three characterizations, *C*Log *P*, retention time in RP-HPLC, and aqueous solubility, indicated that **5** is the most hydrophilic molecule among all the synthesized probes. However, PEG probe **4** gave no successful target tagging result in spite of having the second best aqueous solubility and hydrophobicity. This can possibly be attributed to the abovementioned helical conformation of PEG in an aqueous environment, which lowers the affinity of the pharmacophore with its target. Conversely, the most hydrophobic probe, **1**, provided the best result in target tagging experiments, whereas ethyl tethered **3**, which demonstrated a similar *C*Log *P*, retention time in RP-HPLC, and aqueous solubility to that of probe **1**, was unsuccessful in target tagging analyses. These results suggest that the spatial arrangement of each component (pharmacophore, reactive functionality, molecular tag, and linker) of the probes affected their performance more strongly than aqueous solubility.

However, TAzQ probes **6** and **7** with higher planarity and rigidness than the TAzP linker do not work as expected. The TAzP linker may work more effectively in separating the tag from the pharmacophore, but the decrease in aqueous solubility, which stems from the triazoylquinolyl fragment, canceled this advantage. However, here, we mention a peculiar discrepancy regarding TAzP (**1**). This probe was more soluble in aqueous media than TAzQ (**6** and **7**) even though it showed higher hydrophobicity than TAzQ (Table 1). Unobvious chemical properties can potentially enhance the aqueous solubility of **1** more than expected considering the hydrophobicity.

Aqueous solubility depends on two factors: crystallinity and interactions with water.[32] Hashimoto et al. reported that disruption of molecular planarity and symmetry increase the solubility of drugs.[33] This phenomenon results from a decrease in the efficiency of crystal packing and was consistently observed in drugs with a biaryl moiety. The skewed conformation in biaryl structures confers enhanced solubility in aqueous media because it disrupts the crystal packing. Thus, it is speculated that a skewed conformation around the biaryl linkage of the TAzP linker may improve the aqueous solubility more than expected from the hydrophobicity.

We calculated the dihedral angle of TAzP and triazoylquinolyl model compounds **14** and **15** from the optimized structures obtained by density functional theory (DFT) calculations (B3LYP/6-31G*).[34] The TAzP linker in **1** confers a skewed conformation around the biaryl linkage with the dihedral angle (N1–C1–C1′–C2′) of 13.1°, which was determined from the most stable conformation of **1** in Ref. 14 (Fig. 5). Similar DFT calculation studies gave the dihedral angles of the most stable conformation of **14** and **15**, models of **6** and **7**, respectively (Fig. 5). Expectedly, no twist was observed around the biaryl linkages in **14** ($\theta = 0.0°$) and **15** ($\theta = 0.5°$). Therefore, we suspected that the distinct performance of **1** among the 'CuAAC'-prepared probes can be attributed to such disruption of planarity owing to the skewed conformation around the biaryl linkage (Fig. 5).

In conclusion, TAzP probe **1** afforded greater efficiency in target tagging than probes **3**–**7** because of a combination of high rigidness and good aqueous solubility. The rigid biaryl linker effectively casts the molecular tag away from the pharmacophore and provides improved aqueous solubility in spite of its hydrophobic properties. The enhanced aqueous solubility is suggested to be attributable to the skewed conformation around the biaryl linkage identified in the DFT-calculated structure. Though the aqueous solubility of triglycyl **5** was higher than that of **1**, the flexible triglycyl linker would not afford adequate spatial separation of the tag and

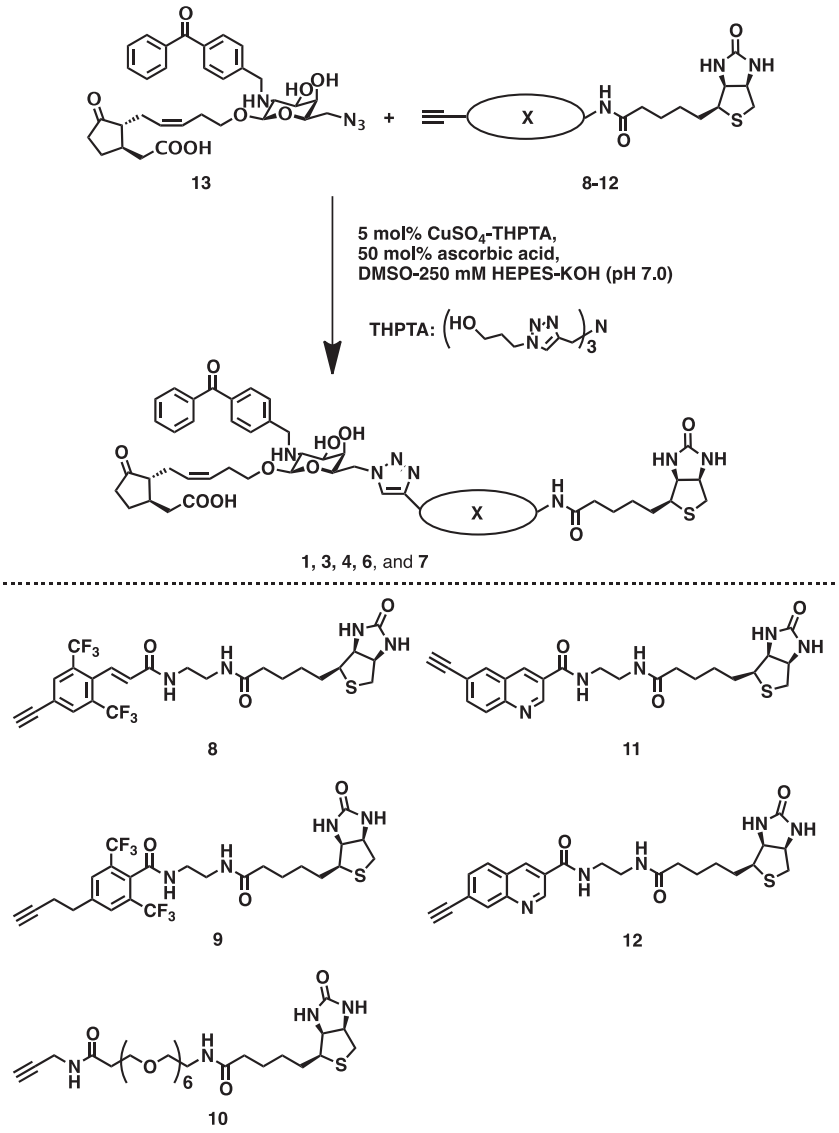

Figure 3. CuAAc coupling of alkyne units **8**–**12** and azide-JAG (**13**)[14] for production of probes **1**, **3**, **4**, **6**, and **7**, respectively.

pharmacophore. The distinguished performance of our TAzP linker offers advantages such as high-performance, aqueous solubility, and synthetic accessibility. The TAzP linker provides a powerful alternative linker system for molecular probe technology.

Furthermore, our results provide a useful guideline for the development of improved linkers. For example, it is already known that *meta*-fluorination of a biaryl structure increases the dihedral angle around the biaryl linkage.[33] Thus, a *m*-fluoro-TAzP adduct can achieve greater aqueous solubility and higher performance as a molecular probe.

Unless otherwise stated, reactions were performed in flame-dried glassware under argon or nitrogen atmosphere using dry solvents. Solvents were dried over activated molecular sieves under argon atmosphere. All starting materials were purchased from commercial sources and used as received, unless otherwise stated. Liquids and solutions were transferred via syringe or a positive-pressure cannula. Brine solutions refer to saturated aqueous sodium chloride solutions. Thin-layer chromatography (TLC) was performed using silica gel 60 F_{254} precoated plates (0.25 mm) and visualized by UV fluorescence quenching or anisaldehyde or $H_3(PMo_{12}O_{40})$ staining. Silica gel 60 N (particle size 63–210 mm) was used for column chromatography. HPLC purifications were performed using PU-2089 with a UV-2075 detector (Jasco Ltd) equipped with Cosmosil 5C18AR (φ 20 × 250 mm, Nakalai. Tesque

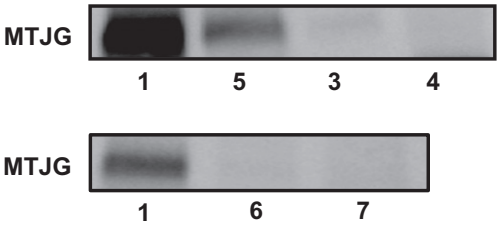

Figure 4. Chemiluminescence detection of MTJG by each probe (**1**, **3**–**7**): Motor cell protoplasts from pulvini of *S. saman* (~1 × 10^4 protoplasts in 0.1 mL) were mixed with each probe (1 × 10^{-4} M). The mixture was incubated for 5 min at 0 °C, and cross-linking was carried out by UV irradiation (365 nm) for 20 min at 4 °C. After centrifugation (110 × *g*, 5 min, 4 °C), the sediment was homogenized with buffer. Centrifugations of lysate (1st: 3000 × *g*, 15 min, 4 °C; 2nd: 100,000 × *g*, 1 h, 4 °C) gave a crude membrane pellet. This pellet was analyzed by SDS–PAGE (7.5–15% gradient gel), and protein bands were detected by LAS-4000 Bioimager (Fuji Film Co., Ltd) using an ECL Advance western blotting detection kit (GE Healthcare UK, Ltd) and analyzed using MultiGauge software (Fuji Film Co., Ltd).

Table 1
Hydrophobic parameters and solubility of synthetic probes (**1** and **3**–**7**)

No	*C*Log*P*	Rt[a] (min) Isocratic	Satd conc (mM)
1	4.89	7.73	0.211
3	5.08	5.70	0.268
4	1.14	2.20	1.057
5	0.32	1.78	55.739
6	3.56	2.35	0.053
7	3.56	2.47	0.082

[a] Column: Eclipse plus C18 narrow bore RRHT 2.1 × 50 mm, flow rate: 0.15 mL/min, isocratic: 33% aq CH_3CN.

Ltd) at the flow rate of 4.0 mL/min. ^1H and ^{13}C NMR spectra were recorded on ECA400 and Alpha 500 spectrometers (Jeol Ltd). Chemical shifts are given in parts per million (ppm) relative to Me_4Si (0.0 ppm). Data for ^1H NMR spectra are reported as follows: chemical shift in ppm; integration, multiplicity, and coupling constants in Hz. Multiplicity and qualifier abbreviations are as follows: s = singlet, d = doublet, t = triplet, q = quartet, quint = quintet, m = multiplet, br = broad. IR spectra were recorded on an FT/IR-410 spectrometer (Jasco Co., Ltd) and are reported as frequency of absorption (cm^{-1}). LR- and HR-MS were recorded in ESI-mode using MicrOTOF-II and APEX-III spectrometers (Bruker Daltonics Ltd). The optical rotation was recorded on a DIP-360 spectrometer using a 100-mm cell. UPLC–MS analysis was performed using an Agilent 1290 Infinity LC (Agilent Ltd) equipped with a MicrOTOF-II (Bruker Daltonics Ltd)

To a solution of azide **13** (1.0 mg, 1.32 μmol) and alkyne unit **9** (1.0 mg, 1.68 μmol) in DMSO/250 mM HEPES buffer (pH 7) (4:1) were added $CuSO_4{\cdot}5H_2O$–THPTA complex (5 mol %) and ascorbic acid (50 mol %). After being shaken for 1 h at 30 °C, the reaction mixture was cooled to rt and successively purified by HPLC (44% MeCN aq containing 0.1% TFA) to give **3** (1.1 mg, 0.928 μmol, 70%).

^1H NMR (500 MHz, CD_3OD) 7.85–7.82 (m, 4 H), 7.79–7.77 (m, 2 H), 7.72 (br, 1 H), 7.68–7.65 (m, 3 H), 7.55–7.52 (m, 2 H), 5.47–5.39 (m, 2 H), 4.66–4.61 (m, 3 H), 4.52–4.48 (m, 3 H), 4.29 (dd, *J* = 8.0, 4.5 Hz, 1 H), 3.95–3.89 (m, 2 H), 3.85 (br, 1 H), 3.69–3.63 (m, 1 H), 3.52–3.45 (m, 3 H), 3.37–3.34 (m, 2 H), 3.25–3.15 (m, 4 H), 3.07–3.04 (m, 2 H), 2.91 (dd, *J* = 12.8, 5.0 Hz, 1 H), 2.69 (d, *J* = 12.8 Hz, 1 H), 2.62 (dd, *J* = 15.0, 3.5 Hz, 1 H), 2.45–2.16 (m, 10 H), 2.05–1.94 (m, 2 H), 1.75–1.30 (m, 6 H), 0.94–0.86 (m, 1 H); IR (film) 3277, 2929, 1672, 1281, 1201, 1178, 1124, 1161, 796, 721, 696 cm^{-1}; $[\alpha]_D^{27}$ − 6.4° (*c* 0.06, DMSO); HRMS (ESI, positive) *m/z* $[M+H]^+$ calcd for $C_{57}H_{67}F_6N_8O_{11}S$, 1185.4554, found 1185.4564.

To a solution of azide **13** (17.5 mg, 20.7 μmol) and alkyne unit **10** (16.9 mg, 27.4 μmol) in DMSO/250 mM HEPES buffer (pH 7) (4:1) were added $CuSO_4{\cdot}5H_2O$–THPTA complex (5 mol %) and ascorbic acid (50 mol %). After being shaken for 1 h at 30 °C, the reaction mixture was cooled to rt and successively purified by HPLC (30% MeCN aq containing 0.1% TFA) to give **4** (20.0 mg, 16.3 μmol, 79%).

^1H NMR (500 MHz, CD_3OD) 7.86–7.85 (m, 3 H), 7.79–7.77 (m, 2 H), 7.67–7.65 (m, 3 H), 7.56–7.53 (m, 2 H), 5.52–5.43 (m, 2 H), 4.66–4.63 (m, 2 H), 4.54–4.40 (m, 4 H), 4.29 (dd, *J* = 8.0, 4.5 Hz, 1 H), 4.02–3.99 (m, 1 H), 3.88 (br, 2 H), 3.79–3.72 (m, 3 H), 3.65–3.60 (m, 22 H), 3.54–3.47 (m, 4 H), 3.22–3.18 (m, 2 H), 2.91 (dd, *J* = 13.0, 5.0 Hz, 1 H), 2.68 (d, *J* = 13.0 Hz, 1 H), 2.65–2.62 (m, 1 H), 2.48–2.45 (m, 2 H), 2.41–2.25 (m, 9 H), 2.22–2.19 (m, 2 H), 2.08–1.97 (m, 2 H), 1.76–1.30 (m, 6 H), 0.96–0.87 (m, 1 H); IR (film) 3278, 3076, 2873, 1659, 1551, 1450, 1279, 1196, 1049, 1023, 1003, 822, 798, 762, 706 cm^{-1}; $[\alpha]_D^{28}$ − 32.1° (*c* 0.19, MeOH); HRMS (ESI, positive) *m/z* $[M+H]^+$ calcd for $C_{60}H_{87}N_8O_{17}S$, 1223.5910, found 1223.5925.

To a solution of azide **13** (3.9 mg, 6.43 μmol) and alkyne unit **11** (3.0 mg, 6.44 μmol) in DMSO/250 mM HEPES buffer (pH 7) (4:1) were added $CuSO_4{\cdot}5H_2O$–THPTA complex (5 mol %) and ascorbic acid (50 mol %). After being shaken for 1 h at 30 °C, the reaction

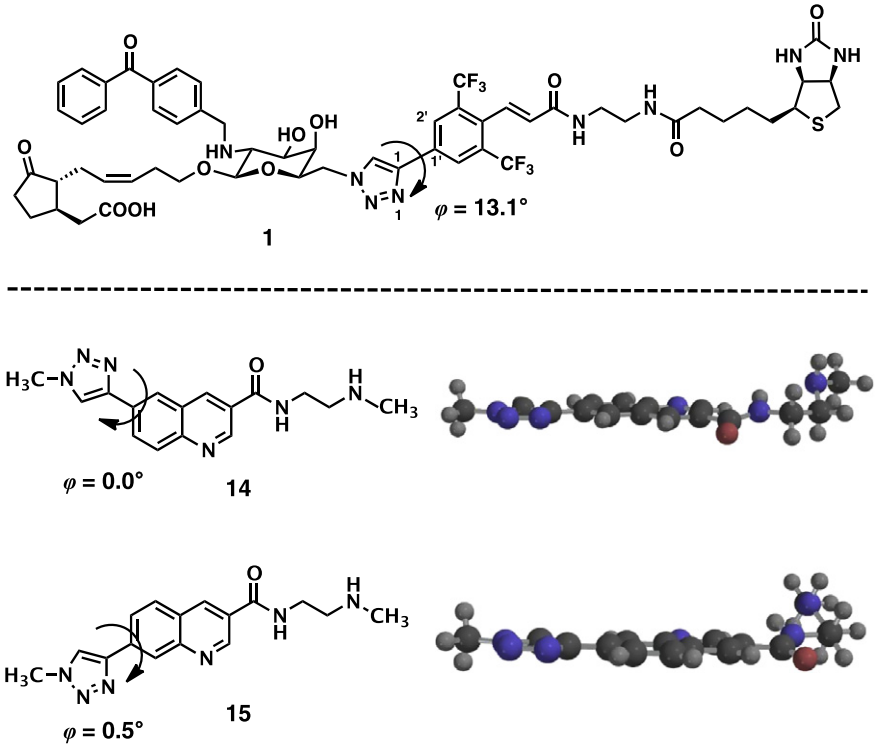

Figure 5. Dihedral angles around the biaryl linkage in TAzP probe (**1**) and TAzQ models (**14** and **15**). Each angle was determined by DFT calculations (B3LYP/6-31G*).

mixture was cooled to rt and successively purified by HPLC (34% MeCN aq containing 0.1% TFA) to give **6** (2.4 mg, 2.24 μmol, 35%).

^{1}H NMR (400 MHz, CD_3OD) 9.24 (d, J = 2.0 Hz, 1 H), 8.84 (d, J = 2.0 Hz, 1 H), 8.57 (s, 1 H), 8.52 (d, J = 2.0 Hz, 1 H), 8.35 (dd, J = 8.8, 2.0 Hz, 1 H), 8.17 (d, J = 8.8 Hz, 1 H), 7.86–7.84 (m, 2 H), 7.79–7.77 (m, 2 H), 7.67–7.65 (m, 3 H), 7.56–7.52 (m, 2 H), 5.38–5.27 (m, 2 H), 4.66 (d, J = 7.8 Hz, 1 H), 4.53 (d, J = 13.2 Hz, 1 H), 4.48 (d, J = 13.2 Hz, 1 H), 4.38 (dd, J = 7.8, 4.4 Hz, 1 H), 4.17–4.08 (m, 2 H), 3.99–3.98 (m, 1 H), 3.94 (dd, J = 11.2, 3.2 Hz, 1 H), 3.70–3.63 (m, 1 H), 3.61–3.58 (m, 2 H), 3.51–3.47 (m, 4 H), 3.34–3.32 (m, 3 H), 3.04–3.00 (m, 1 H), 2.78 (dd, J = 12.8, 4.8 Hz, 1 H), 2.60 (d, J = 12.8 Hz, 1 H), 2.54–2.50 (m, 1 H), 2.39–2.08 (m, 9 H), 1.98–1.82 (m, 2 H), 1.68–1.28 (m, 7 H); ^{13}C NMR (100 MHz, CD_3OD), δ 221.5, 197.6, 176.7, 175.9, 168.0, 166.0, 150.0, 149.4, 147.3, 139.8, 138.4, 137.7, 136.9, 134.1, 131.6 (2C), 131.5 (2C), 131.3, 131.0 (2C), 130.6, 130.2, 129.6 (2C), 129.5, 129.3, 128.8, 128.4, 126.1, 124.8, 100.5, 75.2, 70.5, 69.7, 63.3, 61.6, 59.5, 56.8, 55.1, 53.6, 52.1, 51.3, 41.2, 41.0, 40.0, 39.7, 39.0, 38.7, 36.9, 29.7, 29.5, 28.9, 28.2, 26.9, 26.2; HRMS (ESI, positive) m/z $[M+H]^+$ calcd for $C_{56}H_{66}N_9O_{11}S$, 1072.4602, found 1072.4588.

To a solution of azide **13** (2.0 mg, 3.27 μmol) and alkyne unit **12** (1.3 mg, 2.79 μmol) in DMSO/250 mM HEPES buffer (pH 7) (4:1) were added $CuSO_4{\cdot}5H_2O$–THPTA complex (5 mol %) and ascorbic acid (50 mol %). After being shaken for 1 h at 30 °C, the reaction mixture was cooled to rt and successively purified by HPLC (34% MeCN aq containing 0.1% TFA) to give **7** (1.4 mg, 1.31 μmol, 45%).

^{1}H NMR (400 MHz, CD_3OD) 9.28 (d, J = 2.0 Hz, 1 H), 8.80 (d, J = 2.0 Hz, 1 H), 8.64 (s, 1 H), 8.52 (s, 1 H), 8.23–8.15 (m, 2 H), 7.86–7.84 (m, 2 H), 7.79–7.77 (m, 2 H), 7.67–7.65 (m, 3 H), 7.56–7.52 (m, 2 H), 5.37–5.26 (m, 2 H), 4.67 (d, J = 8.2 Hz, 1 H), 4.53 (d, J = 13.2 Hz, 1 H), 4.48 (d, J = 13.2 Hz, 1 H), 4.38 (dd, J = 8.2, 4.8 Hz, 1 H), 4.15–4.12 (m, 2 H), 3.98–3.98 (m, 1 H), 3.95–3.91 (m, 1 H), 3.69–3.65 (m, 1 H), 3.61–3.58 (m, 2 H), 3.51–3.47 (m, 4 H), 3.34–3.32 (m, 3 H), 3.02–2.96 (m, 1 H), 2.79 (dd, J = 12.8, 5.2 Hz, 1 H), 2.61 (d, J = 12.8 Hz, 1 H), 2.55–2.50 (m, 1 H), 2.26–2.20 (m, 9 H), 2.00–1.84 (m, 2 H), 1.64–1.28 (m, 6 H), 0.96–0.86 (m, 1 H); ^{13}C NMR (100 MHz, CD_3OD), δ 221.8, 197.9, 176.7, 174.6, 168.0, 167.8, 150.0, 149.0, 147.4, 139.7, 139.1, 137.9, 135.2, 134.0, 131.5 (2C), 131.3, 131.0 (2C), 131.0 (2C), 130.6, 130.1, 129.6 (2C), 129.4, 129.2, 128.9, 128.6, 125.1, 123.9, 101.4, 75.1, 70.4, 69.7, 63.3, 61.6, 59.6, 56.9, 55.2, 53.5, 52.2, 51.3, 41.1, 41.0, 39.9, 39.7, 38.9, 38.7, 36.8, 29.7, 29.4, 28.9, 28.2, 26.8, 26.1; HRMS (ESI, positive) m/z $[M+H]^+$ calcd for $C_{56}H_{66}N_9O_{11}S$, 1072.4602, found 1072.4602.

The aqueous solubility of each probe was determined in miliQ at room temperature. MiliQ (20 μL) was added to an excess amount of each probe to prepare a saturated solution. The suspension was kept in an ultrasonic bath for 15 min and vigorously shaken by a vortex mixer for 10 min. Afterwards, the mixture was allowed to stand for 30 min, and the suspension was then centrifuged (4000 rpm, 2 min). The resultant supernatant was transferred to a new tube and centrifuged (15,000 rpm, 3 min) again. Finally, the concentration of the probe in this supernatant was analyzed by UPLC–MS.

Acknowledgments

This work was supported by a Grant-in-Aid for Scientific Research on Innovative Areas 'Chemical Biology of Natural Products' from the Ministry of Education, Culture, Sports, Science and Technology, Japan, and Grants-in-Aid for Scientific Research (No. 23310147), JSPS Bilateral Programs from JSPS, Japan.

Supplementary data

Supplementary data (synthesis of alkyne units and NMR charts of probes) associated with this article can be found, in the online version, at http://dx.doi.org/10.1016/j.bmcl.2012.10.124.

References and notes

1. Ueda, M. *Chem. Lett.* **2012**, *41*, 658.
2. Leslie, B. J.; Hergenrother, P. J. *Chem. Soc. Rev.* **2008**, *37*, 1347.
3. Bottcher, T.; Pitscheider, M.; Sieber, S. A. *Angew. Chem., Int. Ed. Engl.* **2010**, *49*, 2680.
4. Hashimoto, M.; Yang, J.; Holman, G. D. *ChemBioChem* **2001**, *2*, 52.
5. Sato, S.-I.; Kwon, Y.; Kamisuki, S.; Srivastava, N.; Mao, Q.; Kawazoe, Y.; Uesugi, M. *J. Am. Chem. Soc.* **2007**, *129*, 873.
6. Shiyama, T.; Furuya, M.; Yamazaki, A.; Terada, T.; Tanaka, A. *Bioorg. Med. Chem.* **2004**, *12*, 2831.
7. Ueda, M.; Manabe, Y.; Mukai, M. *Bioorg. Med. Chem. Lett.* **2011**, *21*, 1359.
8. Sato, S.; Murata, A.; Shirakawa, T.; Uesugi, M. *Chem. Biol.* **2010**, *17*, 616.
9. Dean, P. M.; Cambridge University Press: Molecular foundations of drug-receptor interaction, 1987.
10. Nakamura, Y.; Miyatake, R.; Ueda, M. *Angew. Chem., Int. Ed. Engl.* **2008**, *47*, 7289.
11. Abuchowski, A.; Mccoy, J. R.; Palczuk, N. C.; Vanes, T.; Davis, F. F. *J. Biol. Chem.* **1977**, *252*, 3582.
12. Harris, J. M. *Poly (Ethylene Glycol) Chemistry Biotechnical and Biomedical Applications*; Springer, 1992.
13. Tamura, T.; Terada, T.; Tanaka, A. *Bioconjug. Chem.* **2003**, *14*, 1222.
14. Nakamura, Y.; Inomata, S.; Ebine, M.; Manabe, Y.; Iwakura, I.; Ueda, M. *Org. Biomol. Chem.* **2011**, *9*, 83.
15. Nakamura, Y.; Mithöfer, A.; Kombrink, E.; Boland, W.; Hamamoto, S.; Uozumi, N.; Tohma, K.; Ueda, M. *Plant Physiol.* **2011**, *155*, 1226.
16. Ueda, M.; Okazaki, M.; Ueda, K.; Yamamura, S. *Tetrahedron* **2000**, *56*, 8101.
17. Meldal, M.; Tornoe, C. W. *Chem. Rev.* **2008**, *108*, 2952.
18. Tornøe, C. W.; Christensen, C.; Meldal, M. *J. Org. Chem.* **2002**, *67*, 3057.
19. Kolb, H. C.; Finn, M. G.; Sharpless, K. B. *Angew. Chem., Int. Ed. Engl.* **2004**, *2001*, 40.
20. Ueda, M.; Yang, G.; Ishimaru, Y.; Itabashi, T.; Tamura, S.; Kiyota, H.; Kuwahara, S.; Inomata, S.; Shoji, M.; Sugai, T. *Bioorg. Med. Chem.* **2012**, *20*, 5832.
21. Hong, V.; Presolski, S. I.; Ma, C.; Finn, M. G. *Angew. Chem., Int. Ed. Engl.* **2009**, *48*, 9879.
22. Chan, T. R.; Hilgraf, R.; Sharpless, K. B.; Fokin, V. V. *Org. Lett.* **2004**, *6*, 2853.
23. Fujita, Y.; Yonehara, M.; Tetsuhashi, M.; Noguchi-Yachide, T.; Hashimoto, Y.; Ishikawa, M. *Bioorg. Med. Chem.* **2010**, *18*, 1194.
24. Ueda, M.; Yamamura, S. *Angew. Chem., Int. Ed. Engl.* **2000**, *39*, 1400.
25. Ueda, M.; Nakamura, Y. *Nat. Prod. Rep.* **2006**, *23*, 548.
26. Anderson, P. M.; Wilson, M. R. *Mol. Phys.* **2005**, *103*, 89.
27. Xue, Y.; O'Mara, M. L.; Surawski, P. P. T.; Trau, M.; Mark, A. E. *Langmuir* **2011**, *27*, 296.
28. Wahab, S. A.; Matsuura, H. *PCCP* **2001**, *3*, 4689.
29. Hansch, C.; Quinlan, J. E.; Lawrence, G. L. *J. Org. Chem.* **1968**, *33*, 347.
30. Valvani, S. C.; Yalkowsky, S. H.; Roseman, T. J. *J. Pharm. Sci.* **1981**, *70*, 502.
31. *CLOGP* of each probe was estimated from OSIRIS property explorer (http://www.chemexper.com/tools/propertyExplorer/main.html).
32. Jain, N.; Yalkowsky, S. H. *J. Pharm. Sci.* **2001**, *90*, 234.
33. Ishikawa, M.; Hashimoto, Y. *J. Med. Chem.* **2011**, *54*, 1539.
34. GAUSSIAN 03 (Revision D.02): Frisch, M. J.; Trucks, G. W.; Schlegel, H. B.; Scuseria, G. E.; Robb, M. A.; Cheeseman, J. R.; Montgomery, J. A., Jr.; Vreven, T.; Kudin, K. N.; Burant, J. C.; Millam, J. M.; Iyengar, S. S.; Tomasi, J.; Barone, V.; Mennucci, B.; Cossi, M.; Scalmani, G.; Rega, N.; Petersson, G. A.; Nakatsuji, H.; Hada, M.; Ehara, M.; Toyota, K.; Fukuda, R.; Hasegawa, J.; Ishida, M.; Nakajima, T.; Honda, Y.; Kitao, O.; Nakai, H.; Klene, M.; Li, X.; Knox, J. E.; Hratchian, H. P.; Cross, J. B.; Bakken, V.; Adamo, C.; Jaramillo, J.; Gomperts, R.; Stratmann, R. E.; Yazyev, O.; Austin, A. J.; Cammi, R.; Pomelli, C.; Ochterski, J. W.; Ayala, P. Y.; Morokuma, K.; Voth, G. A.; Salvador, P.; Dannenberg, J. J.; Zakrzewski, V. G.; Dapprich, S.; Daniels, A. D.; Strain, M. C.; Farkas, O.; Malick, D. K.; Rabuck, A. D.; Raghavachari, K.; Foresman, J. B.; Ortiz, J. V.; Cui, Q.; Baboul, A. G.; Clifford, S.; Cioslowski, J.; Stefanov, B. B.; Liu, G.; Liashenko, A.; Piskorz, P.; Komaromi, I.; Martin, R. L.; Fox, D. J.; Keith, T.; Al-Laham, M. A.; Peng, C. Y.; Nanayakkara, A.; Challacombe, M.; Gill, P. M. W.; Johnson, B.; Chen, W.; Wong, M. W.; Gonzalez, C.; Pople, J. A. GAUSSIAN, Inc., Wallingford CT, 2004.